Available online at www.sciencedirect.com

SCIENCE DIRECT®

Journal of Magnetic Resonance 168 (2004) 132–136

JMR Journal of Magnetic Resonance

www.elsevier.com/locate/jmr

Electron spin-relaxation via vibronic level of nickel (I) and nickel (III) cyanide complexes in NaCl single crystals

N.V. Vugman,[a,*] M.B. de Araújo,[a] N.M. Pinhal,[a] C.J. Magon,[b] and A.J. da Costa Filho[b]

[a] *Instituto de Física—Universidade Federal do Rio de Janeiro, Rio de Janeiro, RJ 21910-240, Brazil*
[b] *Instituto de Física, Universidade de São Paulo, USP, São Carlos, SP 13560-970, Brazil*

Received 12 September 2003; revised 5 February 2004

Abstract

Electron spin–lattice relaxation rates for the low spin $[Ni(CN)_4]^{1-}$ and $[Ni(CN)_4]^{3-}$ complexes in NaCl host lattice were measured by the inversion recovery technique in the temperature range 7–50 K. The data for both paramagnetic species fit very well to a relaxation process involving localized anharmonic vibration modes, also responsible for the g-tensor temperature dependence.

Keywords: Spin relaxation; Vibronic process; Nickel complexes; Magnetic resonance

1. Introduction

Electron paramagnetic resonance (EPR) spectroscopy has been widely used to study several new paramagnetic species obtained by radiation damage in transition metal cyanides complexes diluted in alkali halide host lattices [1]. The impurity complexes enter the host lattice substituting a corresponding $[AH_n]^{n-1}$ alkali halide cluster. Charge compensation is provided by the formation of positive ion vacancies. These vacancies are known to play an important role in the properties measured by EPR spectroscopy [2–4], as well as in infrared spectroscopy [5].

It is well established that, upon irradiation, hexacoordinated metal complexes are reduced by the capture of an electron in a metal–ligand antibonding orbital. Tetracoordinated complexes, in contrast, are both oxidized and reduced. In the case of $[Ni(CN)_4]^{2-}$, irradiation results in concomitant formation of two paramagnetic species, $[Ni(CN)_4]^{1-}$ and $[Ni(CN)_4]^{3-}$, having, respectively, d^7 configuration with one unpaired electron in a d_{z^2} orbital and d^9 configuration, with one unpaired electron in a $d_{x^2-y^2}$ orbital. This is the case, for example, of $[Ni(CN)_4]^{2-}$ inserted in a NaCl host lattice and submitted to ionizing radiation: the simultaneous observation of these two well characterized species is specially suited [6] for comparative studies of temperature effects; the mechanism of formation of these species, an intriguing unknown since the early works on these species, [7,8] has been recently unraveled through the study of the kinetics of formation of these species in single crystals of NaCl doped with $[Ni(CN)_4]^{2-}$ as a function of the radiation doses and after-irradiation time [9].

On the other hand, the interesting g-tensor behavior, measured by CW EPR as a function of the temperature [6], lead us to postulate the presence of localized anharmonic vibrations for both paramagnetic species and, with the aid of a simple crystal field model, to estimate the frequencies of these vibration modes.

Low frequency vibrational modes were invoked in the literature to explain electron spin–lattice relaxation of defects in crystalline quartz [10] and of atomic-hydrogen centers generated in fused silica by γ-irradiation [11]. Recently, it was shown that localized modes with energies in the range of 130–240 cm^{-1} are contributing for the spin–lattice relaxation for the $S = 1/2$ transition metal complexes [12].

Electron spin–lattice relaxation studies, performed by pulsed EPR, added important information on the presence of localized vibration modes for paramagnetic rhodium cyanides as impurities in alkali halide host lattices [13]. In this work we report electron spin–lattice relaxation measurements on the two paramagnetic

---

[*] Corresponding author. Fax: +55-21-2275-9717.
E-mail address: ney@if.ufrj.br (N.V. Vugman).

doi:10.1016/j.jmr.2004.02.005

complexes formed when $[Ni(CN)_4]^{2-}$ in NaCl host lattice is submitted to ionizing radiation, aiming to test the efficiency of the vibronic electron spin–lattice relaxation process also for nickel complexes.

2. Experimental

Single crystals of NaCl doped with $[Ni(CN)_4]^{2-}$ were grown at room temperature by slow evaporation of an aqueous solution to which $K_2Ni(CN)_4$ was added in 0.5% molar proportion. They were of about 3-mm edge and the best ones were chosen by visual inspection. The crystals were irradiated for 20 min, at room temperature, with a tungsten X-rays source operating at 80 kV and 5 mA.

Pulsed EPR measurements were performed in a Bruker ELEXSYS E580 in the 7–50 K temperature range. Electron spin–lattice relaxation times were measured using an inversion recovery (IR) technique. The pulse sequence employed was a 32 ns inversion pulse followed by a 16–32 ns detection sequence. Detection was carried out on the top of the echo. Samples are diluted enough to avoid additional non-isolated paramagnetic species due to cluster formation whose spectral lines could contribute to diffusion during pulse action.

3. Results

Figs. 1a and b compare a typical X-band spectrum observed with the external magnetic field parallel to one of the NaCl crystallographic axes and a Q-band spectrum taken at the same orientation. With the sample aligned in this way, both the parallel and the perpendicular features of the spectrum are measured in the same magnetic field scan. The two paramagnetic species mentioned above are clearly assigned. At Q-band it is possible to observe a third species, similar to the oxidized one, superimposed to this species at X-band. The arrows indicate the four lines used for inversion-recovery measurements, at the parallel and perpendicular features of the two species (lines A and B and lines C and D, respectively). In the previous experiment on $[Rh(CN)_6]^{4-}$ species [13] saturation recovery-cw and inversion recovery gave the same relaxation times indicating any spectral diffusion. Similar conditions for the niquel species allow the measured inversion-recovery times as the true times for relaxation.

Measured relaxation rates as a function of the inverse temperature for the reduced species are shown in Figs. 2A and B in a semilog plot. Analogous measurements for the oxidized species are shown in Fig. 3A and B.

The data behavior is very similar in both cases. Three distinct regions may be observed. A linear behavior is noticed at the higher and medium temperature ranges and a non-linear behavior is observed for the low temperature range.

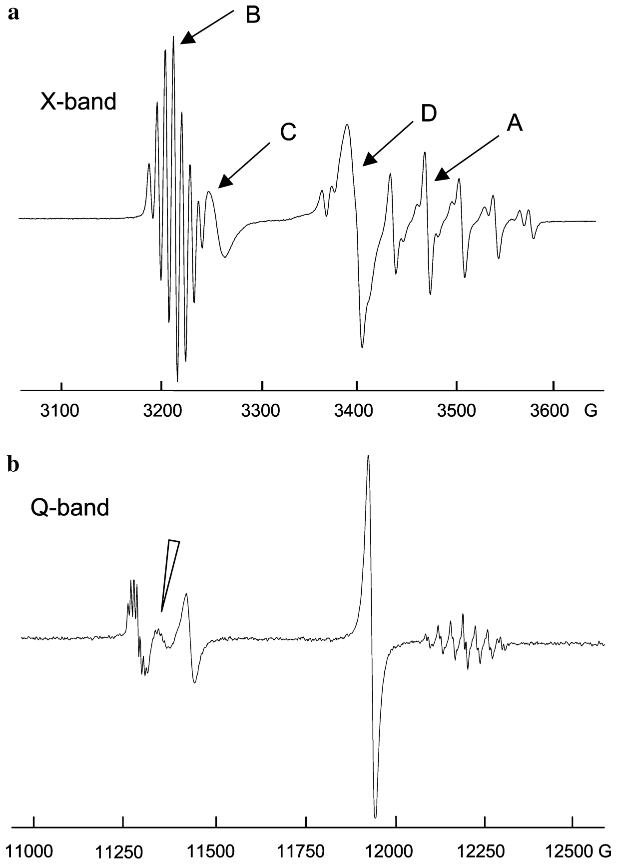

Fig. 1. Room temperature CW EPR spectra at 9.671 GHz (X-band, A) and at 34.28 GHz (Q-band, B). The inversion recovery measurements were performed on lines A, B (parallel and perpendicular spectra of the oxidized species) and on lines C, D (parallel and perpendicular spectra of the reduced species). The mark on B indicates the presence of a second d^7 species.

4. Discussion

A linear behavior in a semilog plot strongly suggests an exponential dependence of the relaxation rate with the inverse of the temperature. A vibronic electron spin–lattice relaxation process, which results in such exponential dependence, has been postulated earlier [13] in order to explain the temperature behavior of $[Rh(CN)_6]^{4-}$ in a KCl host lattice. The model is based on the fact that molecular impurities in a host lattice preserve their vibration modes (localized vibrations) and on the assumption that the temperature dependence of the electron spin–lattice relaxation time would be dominated by the vibrational properties of the defect. The localized vibrations have been shown to be anharmonic with a rather large vibrational amplitude [6]. Under these circumstances, lattice vibrations could beat the localized vibrations producing a difference frequency

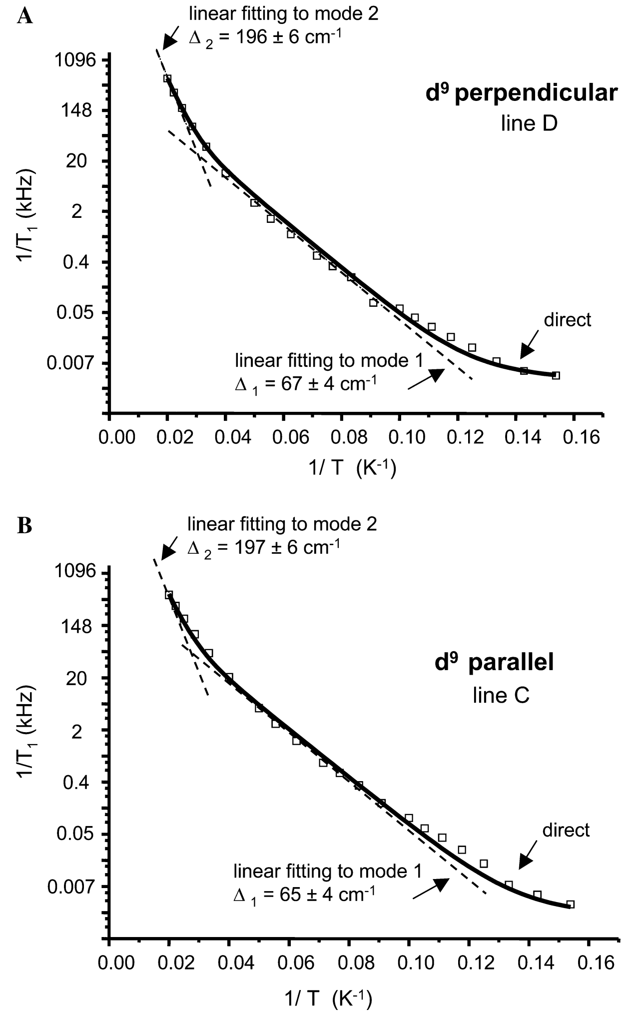

Fig. 2. Semilog plot of the spin–lattice relaxation rates measured from inversion recovery experiments as a function of the inverse of the temperature for the perpendicular and parallel features of the reduced species, lines D and C in the CW spectrum. Dashed lines indicate possibilities of linear fittings. The contribution of the direct process is indicated by an arrow at the lowest temperatures.

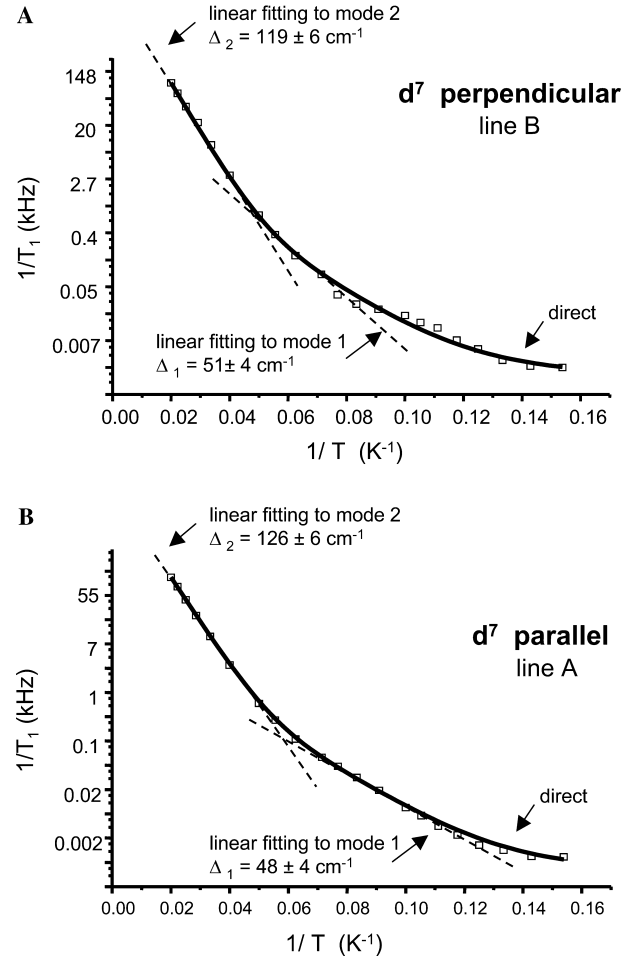

Fig. 3. Semilog plot of the spin–lattice relaxation rates measured from inversion recovery experiments as a function of the inverse of the temperature for the perpendicular and parallel features of the oxidized species, lines B and A in the CW spectrum. Dashed lines indicate possibilities of linear fittings. The contribution of the direct process is indicated by an arrow at the lowest temperatures. The apparent slight anisotropy in the energies of the vibration mode are within the experimental error.

resulting in a spin transition, in a process similar to Murphy's relaxation [14] but in a single well.

The expected temperature dependence for the spin–lattice relaxation rate, as the population of the vibronic levels is determined by the Boltzmann statistics [13], follows an exponential law, independently of how many of the possible vibration modes of frequency Δ_i/h are contributing to the relaxation process. A combined decay remains exponential while the rate constants for the electron spin–lattice relaxations add. So we are measuring a resultant relaxation rate, which, in the present case, is completely dominated by the contribution of the most effective frequency mode at a particular temperature range. However, in order to fit the experimental data in the entire temperature range using a single function, we write the fitting function as a sum of exponentials, each of them is predominating in the temperature region where the respective vibration mode is the most effective. The pre-exponential factors, in this way, loose physical meaning. The fitting function is as follows:

$$1/\mathrm{T}_1 = \sum \mathrm{A}_i \exp(-\Delta_i/kT). \qquad (1)$$

Fitting of the four sets of experimental data to function (1) results in a very good agreement between data and model. Small disagreement appears only at the low temperature region, where the addition of a small contribution of the direct process (of the order of 10^{-4} T) solves the problem.

Raman processes have been fully tested. The best fitting with T^7, T^9 or T^n processes are shown in Fig. 4; they do not agree with the experimental data.

As mentioned in Section 1 of this report, low frequency localized anharmonic modes were inferred from

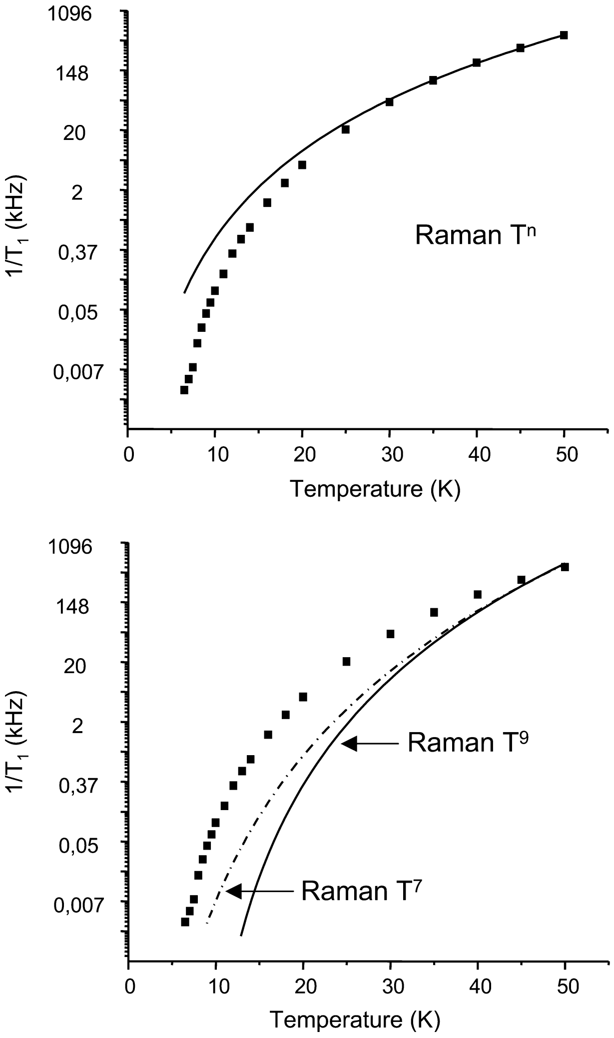

Fig. 4. Semilog plot of the spin–lattice relaxation rates measured from inversion recovery experiments as a function of the temperature for line C in the CW spectrum. Bottom, fitting with a T^9 and a T^7 Raman processes. Top, fitting with a T^n process, the best fitting was achieved with $n = 4.2$.

the g-tensor temperature dependence, for the paramagnetic species under study. Table 1 summarizes the vibration energies got from CW EPR spectroscopy and the same energies derived from the measured spin–lattice relaxation rates.

Table 1
Vibration energies as taken from CW EPR and spin relaxation measurements

Species	CW* A_{1g} mode Inversion recovery (cm^{-1})	CW* B_{1g} mode Inversion recovery (cm^{-1})
Oxidized	$92 \pm 9^*$	
	49 ± 4	126 ± 6
Reduced	$69 \pm 7^*$	$194 \pm 15^*$
	66 ± 4	195 ± 6

* Data from reference [6].

For the reduced species there is an excellent agreement between data taken from g-values and those derived independently from spin relaxation. A similar agreement was found for the $[Rh(CN)_6]^{4-}$ complex in KCl host lattice [13]. In that first paper on this subject we declared that the agreement could be rather fortuitous considering all the simplifying assumptions involved in the localized anharmonic vibrations model and the experimental uncertainties. In face of the present results we are lead to abandon the fortuity hypothesis and believe that both techniques are in fact giving the same results.

For the oxidized species we must consider that the results published in reference [6] were the best fitting we could get at that time. We were not able to separate the two vibration modes as suggested by the theory. The spin relaxation data, however, clearly indicate the presence of two vibration modes. Their averaged energy is the same as that attributed by CW spectroscopy for the A_{1g} vibration mode acting alone. On the other hand, returning to Figs. 1 and 3, we notice that Q-band reveals a low intensity oxidized species, marked by a triangular sign in Fig. 1b. This species is the same as the main oxidized one, differing only by the location of the charge compensating vacancies [9] and is slightly interfering in the relaxation data taken from line B. The existence of this species probably contributes for the lower quality of the g-values fit in CW EPR. Pulsed EPR, more selective to species superimposition than CW EPR, minimize the effect of this superimposition in the relaxation data.

Acknowledgments

The authors are indebted to Conselho Nacional de Desenvolvimento Científico e Tecnológico, CNPq, for a research fellowship (NVV) and for a PhD fellowship (MBA). We are also grateful to Fundação de Amparo à Pesquisa do Estado de São Paulo, FAPESP.

References

[1] For an early review see N.V. Vugman, V.K. Jain, Rev. Roum. Phys. 33 (4–6) (1988) 981.
[2] R.G. Hayes, J. Chem. Phys. 47 (5) (1967) 1692.
[3] R.P.A. Muniz, N.V. Vugman, J. Danon, J. Chem. Phys. 54 (3) (1971) 1284.
[4] N.V. Vugman, A.M. Rossi, J. Danon, J. Chem. Phys. 68 (7) (1978) 3152.
[5] L.H. Jones, J. Chem. Phys. 36 (1962) 1400.
[6] N.V. Vugman, M. Rothier Amaral Jr, Phys. Rev. 42 (1990) 9837.
[7] S.C. Jain, K.V. Reddy, C.L. Gupta, T.Rs. Reddy, Chem. Phys. Lett. 21 (1) (1973) 150.
[8] S.I. Zanette, A.O. Caride, J. Danon, Chem. Phys. 64 (8) (1976) 3381.

[9] M. Braga, N.M. Pinhal, N.V. Vugman, Radiat. Phys. Chem. (Oxford) 64 (2002) 389.
[10] J.G. Castle Jr, D.W. Feldman, Phys. Rev. A 137 (1965) 671.
[11] D.W. Feldman, J.G. Castle Jr, G.R. Wagner, Phys. Rev. 145 (1966) 237.
[12] Y. Zhou, B.E. Bowler, G.R. Eaton, S.S. Eaton, J. Mag. Res. 139 (1999) 165.
[13] J.A. Coelho Neto, N.V. Vugman, J. Mag. Res. B 150 (2) (2001) 105.
[14] J. Murphy, Phys. Rev. 145 (1966) 241.